LAWRENCE
LIVERMORE
NATIONAL
LABORATORY

An internal report: Electron Spectroscopy of the Oxidation and Aging of U and Pu

J. G. Tobin

May 6, 2015

Disclaimer

This document was prepared as an account of work sponsored by an agency of the United States government. Neither the United States government nor Lawrence Livermore National Security, LLC, nor any of their employees makes any warranty, expressed or implied, or assumes any legal liability or responsibility for the accuracy, completeness, or usefulness of any information, apparatus, product, or process disclosed, or represents that its use would not infringe privately owned rights. Reference herein to any specific commercial product, process, or service by trade name, trademark, manufacturer, or otherwise does not necessarily constitute or imply its endorsement, recommendation, or favoring by the United States government or Lawrence Livermore National Security, LLC. The views and opinions of authors expressed herein do not necessarily state or reflect those of the United States government or Lawrence Livermore National Security, LLC, and shall not be used for advertising or product endorsement purposes.

An internal report:
Electron Spectroscopy of the Oxidation and Aging of U and Pu

JG Tobin
Lawrence Livermore National Laboratory
Livermore, CA, USA   94550
Corresponding email:Tobin1@LLNL.Gov

Abstract

Uranium and Plutonium are highly reactive elements that undergo not only chemical reactions but also nuclear reactions. This can lead to possibly significant materials degradation, a matter of potentially great concern. Here, the issue of the electronic structure changes that occur with oxidation and radiological aging will be addressed, in a fairly empirical manner. In essence, the sensitivity of various electron spectroscopic techniques to oxidation and aging will be surveyed and discussed, including the apparent limitations. It will be found that 5d and 4d X-ray absorption and electron energy loss are essentially blind to the changes corresponding to oxidation and aging in U and Pu.

Introduction

Because of the nuclear test ban, the United States of America has sought to maintain the quality of its nuclear deterrent [1] via Science-based Stockpile Stewardship. [2] The first results of the Science-based Stockpile Stewardship Program indicate a robust nature to the nuclear materials with a lifetime in decades. [2,3] However, continued vigilance is prudent. [2,3] With that issue in mind, the question arises concerning the best spectroscopic approach to monitor electronic structure changes in U and Pu, with oxidation and aging. While electronic structure may seem to some to be a secondary issue to structural changes, the electronic structure is a key to understanding the chemical bonding. An understanding of chemical bonding underpins the ability to computationally simulate these materials and thus successfully predict the chemical and materials properties over decades. Thus, in order to predict how these materials will fare over the years ahead, the simulations must be benchmarked with the proper spectroscopic techniques.

Rather than indulge in a discussion of the various merits of the different electron spectroscopies, it is proposed here to take a fairly empirical approach. The central question in each case will be the following: can the spectroscopy in question measure a

An internal report:
Electron Spectroscopy of the Oxidation and Aging of U and Pu

statistically meaningful change associated with material and the corresponding physical or chemical variation? Examples from the literature will be presented and evaluated. In general, discussions of the meaning of the spectroscopic changes will be left to the source articles: here the goal is to evaluate the spectroscopies solely in terms of their sensitivities.
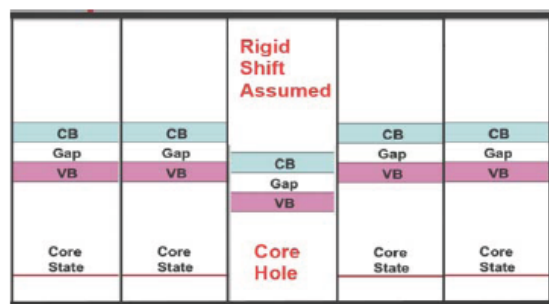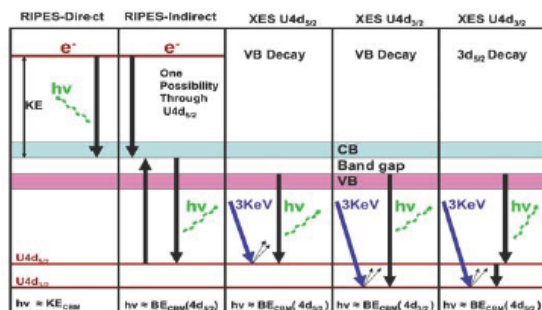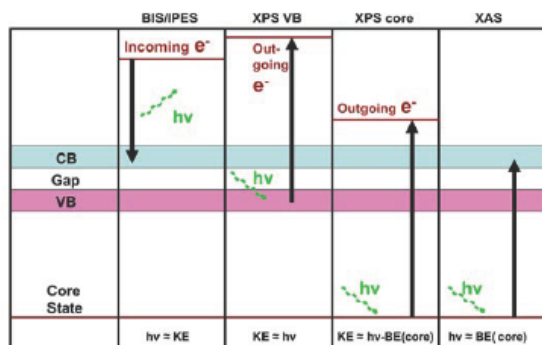
General Discussion

To begin, consider the diagrams in Figure 1. Here, the diagrams are applicable to something like uranium dioxide, with an occupied Valence Band (VB), an unoccupied Conduction Band (CB) and a gap between them. In metals, there would be no gap, but the notation of an occupied VB and unoccupied CB would be retained. The most powerful measurements are often the simplest. For example, by bombarding the sample with X-rays, one can get a measure of the occupied states from X-Ray Photoelectron Spectroscopy. XPS can extract electrons from both core levels and the valence bands. While the XPS of the core levels can provide detailed information, such as the differentiation of the alpha and delta phases of Pu [4,5] shown in Figure 2, this avenue of interrogation will not be pursued here. Instead, the discussion of XPS and its related techniques will focus on the valence band measurements.

Figure 1
Some of the spectroscopic processes are shown here, for the UO$_2$ system.

An internal report:
Electron Spectroscopy of the Oxidation and Aging of U and Pu
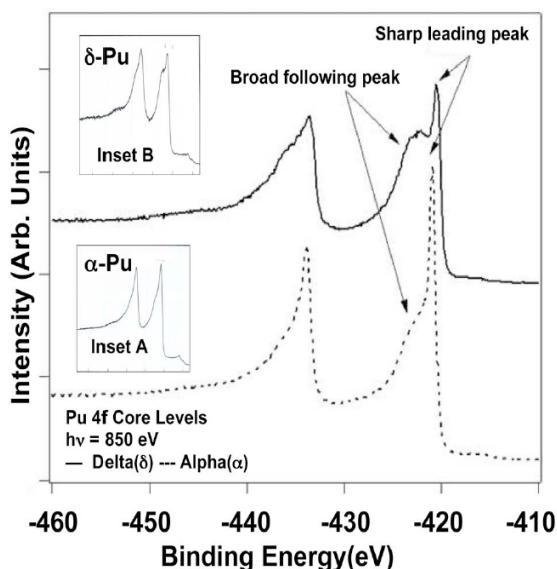

Figure 2
Here are shown 4f core level photoelectron spectra of alpha and delta Pu, using synchrotron radiation at 850 eV. Both alpha and delta peaks are composed of two features: a sharp leading peak and a broad following peak. The alpha and delta spectra differ mainly in terms of the relative magnitudes of the leading and following peaks. Note the strong similarity of these spectra to those collected years earlier (Insets A and B) using Al Kα radiation (1487 eV) , from Neagale. [5]

The corresponding measurement of the unoccupied Conduction Band is Bremsstrahlung Isochromat Spectroscopy (BIS, at high energies) or Inverse Photoelectron Spectroscopy (IPES, more generally). Because the final state in XPS is +1 and the final state in BIS/IPES is -1, and other differences [6], these two techniques are not quite the time reversals of each other. However, they are closely related. Another way to get a measure of

the conduction band is X-ray Absorption Spectroscopy (XAS) and its cousin, Electron Energy Loss Spectroscopy (EELS). At very high energies for the primary electron excitation beam, EELS becomes essentially the same as XAS. [7-9] An interesting and important variant of Photoelectron Spectroscopy (PES) and IPES is the resonant version of each: Resonant PES or RESPES and Resonant IPES or RIPES. The case of RIPES is shown in Figure 1. In both cases, a second indirect channel opens up, going through a core level. Additionally, X-ray Emission Spectroscopy will also be discussed. Several examples of XES decay are shown schematically in Figure 1. While XES can provide a measure of the occupied density of states (ODOS), it is the ODOS in the presence of a core hole. A core hole can produce an effective nuclear charge increase of 1. In the actinides, a $\Delta Z = 1$ can shift the energies of fairly shallow core states (e.g. 4d, 4f, 5p) by as much as 10 to 30 eV. [10] Thus, the low-lying unoccupied density of states (UDOS) can become filled and the XES can provide a measure of the low-lying UDOS in the initial state, before the generation of the core hole. This effect is illustrated in the lowest panel of Figure 1.
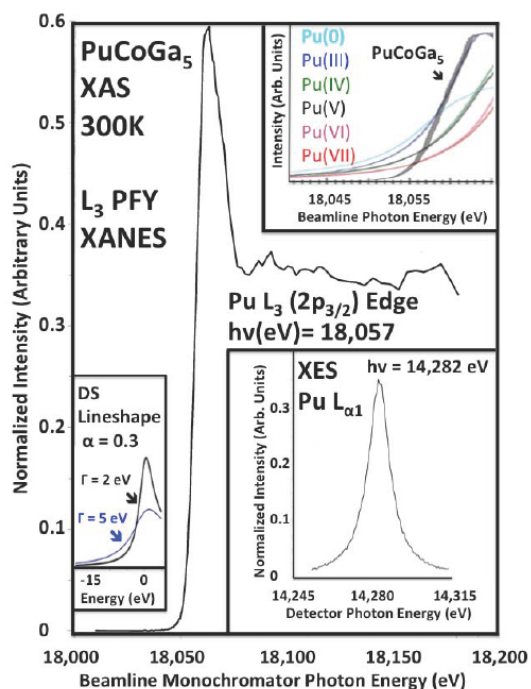
Figure 3
High resolution PFY XAS and XES of Pu. These data were collected at SSRL on Beamline 6-2 in March of 2015. [13] The additional data in the top right inset is from Conradson et al. [16,17]

The XAS measurements to be discussed will encompass transitions into both the 5f UDOS [7,8] and the 6d UDOS of the uranium and plutonium moieties, in particular the new, higher resolution measurements of the $L_3(2p_{3/2})$ edge. [11,12] An example of this higher resolution is shown in Figure 3. Here, the Partial Fluorescence Yield (PFY) XAS measurements at the Pu L_3 edge of PuCoGa$_5$ [13] have been made with a new high resolution X-ray spectrometer. [14] As shown in the inset in the lower right corner,

this X-ray spectrometer can resolve XES spectra of features such as the Pu $L_{\alpha 1}$ line. The earlier technology, based upon multi element Ge solid-state detectors, [15] would average over features such as this. In fact, the Ge solid-state devices can be considered to be almost Total Fluorescence Yield (TFY) detectors. The effect of these different measurement processes can be seen in the inset in the upper right corner of Figure 3. In this inset, the Pu PFY result is compared to earlier work by Conradson et al. [16,17], for a series of Pu oxidation states. The PuCoGa$_5$ PFY spectrum edge jump has been aligned and normalized to the Conradson spectrum for Pu(III). This is not completely arbitrary: it has been shown that (1) the he magnetic susceptibility of PuCoGa$_5$ is indicative of local-moment behavior close to that expected for Pu^{3+};[18] and (2) there appear to be 5 electrons of 5f character in the system. [19]

It is clear that the Conradson data has a much wider edge jump, for all of the Pu oxidation states shown. This wider edge jump can be modeled using a Doniach-Sunjic Lineshape [20], which permits the inclusion of the white line at the edge jump. An example of this modeling is shown in the inset in the lower left part of Figure 3.

An internal report:
Electron Spectroscopy of the Oxidation and Aging of U and Pu

Two simulated spectra are shown, both having an asymmetery (α) of 0.3, but with different lifetime broadenings, Γ. Γ is the half-width-at-half maximum of the Lorentzian part of the DS lineshape. The Γ = 5 eV case would correspond to the averaging over the Pu $L_{\alpha 1}$ peak shown in the lower right inset, while the Γ = 2 eV case would correspond to the improved resolution using the PFY detection. [20] (Note that the normalization here is different than that in the upper right inset. Here, it is the standard mathematical normalization for DS lineshapes.) Again clearly, the sharpening of the edge jump is obtained.

The specifics of the comparison will be couched in terms of answering the following question: Can the spectroscopy under consideration differentiate the two materials, based upon the electronic structure changes? The pairs of materials will be: U vs Pu; U vs UO_2; Pu vs PuO_2; UO_2 vs UO_3, UO_2 vs UF_4; α-Pu vs δ-Pu; and New vs. Radiologically Aged Pu. The techniques will include: XPS and related techniques; $O_{4,5}(5d)$ XAS/EELS; $N_{4,5}(4d)$ XAS/EELS; $L_3(2p_{3/2})$ XAS/XANES; BIS/IPES and XES. Now, the individual cases will be considered.
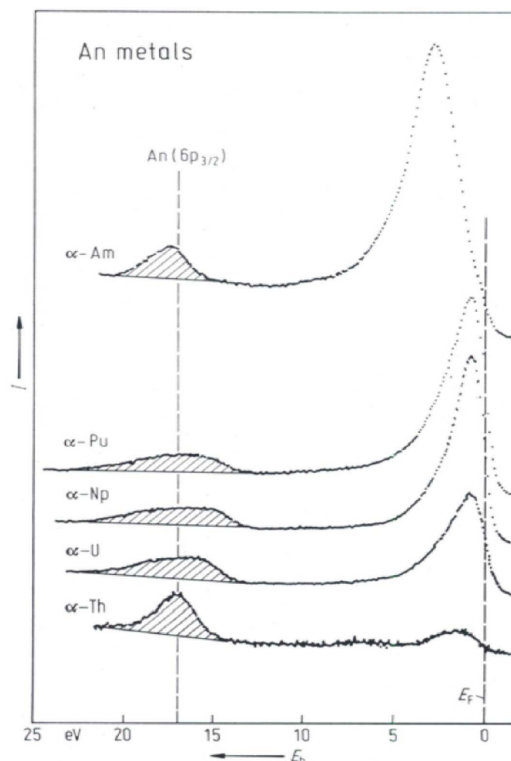
XPS of An and AnOxides

Figure 4a
Valence Band XPS spectra of Th, U, Np, Pu and Am from J. R. Naegele. [5]E_b is the binding energy in eV relative to the Fermi Energy at 0.
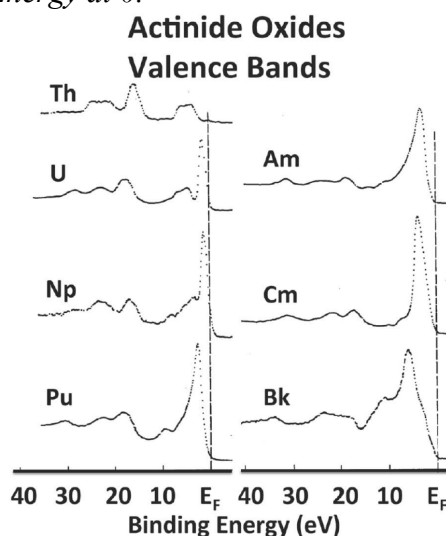

Figure 4b
Valence band region of the oxides of the actinides, Th, U, Np, Pu, Am, Cm, and Bk. [10]

A consideration of Figure 4 rapidly brings one to the conclusion that, in terms of valence band changes, it is easy to distinguish Pu from U, U from uranium oxide and Pu from plutonium oxide.

Furthermore, it has also been shown that PuO_2 and Pu_2O_3 are distinguishable [21] as are UO_2 and UO_3, as shown in Figure 5, which will be discussed in the next section. [22-26]

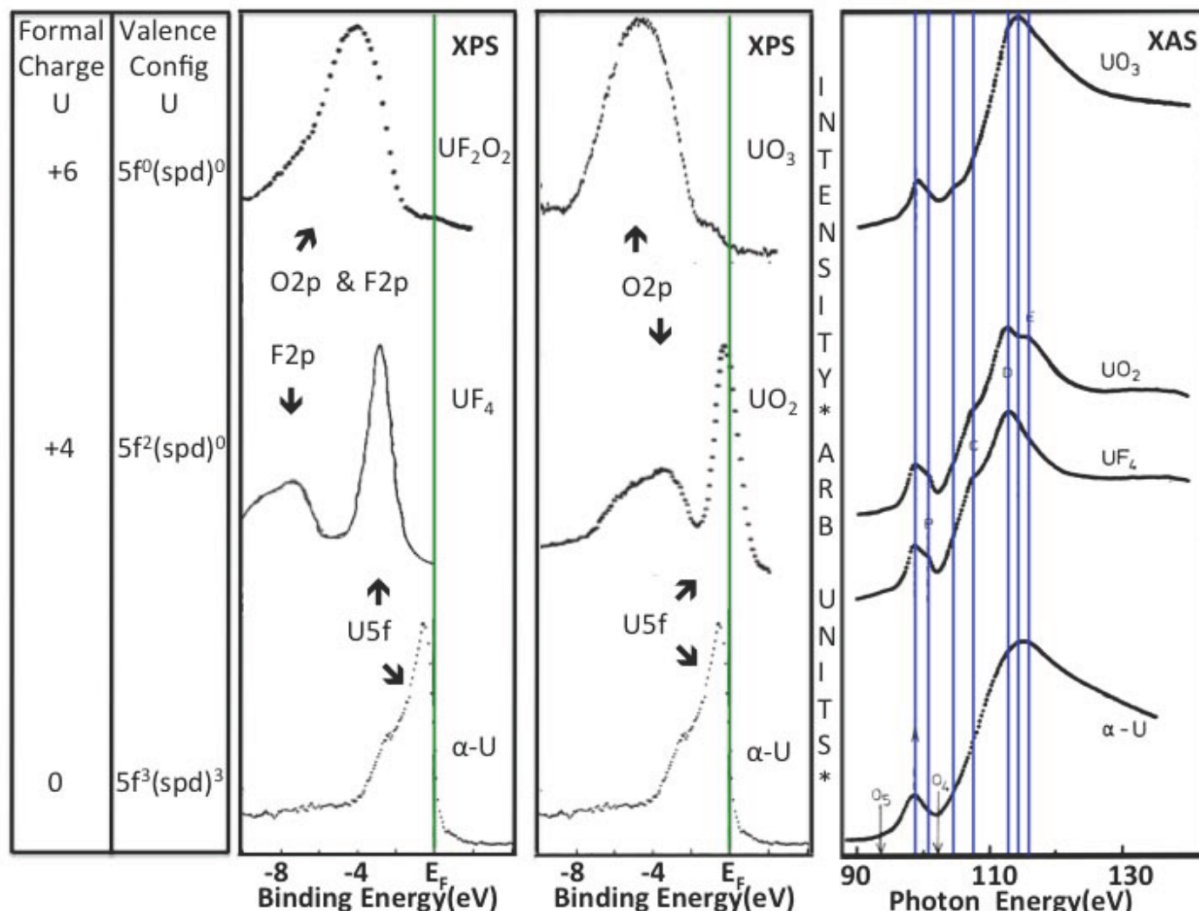## XPS and $O_{4,5}(5d_{5/2}, 5d_{3/2})$ XAS of U, UO_2, UF_4 and UO_3

Figure 5
Here is a comparison of the Formal charge, valence configuration, XPS and 5d XAS of α-U, UO_2, UF_4, UO_3 and UF_2O_2, taken from Reference 22. E_F is the Fermi Energy. The XAS data are from Kalkowski, Kaindl, Brewer and Krone. [23] Except for the UF_4, all of the XPS data are from Veal and coworkers. [10] The UF_4 XPS data are from Thibaut et al., [24] with confirmation by Teterin and coworkers. [25,26]

Again, a consideration of the data leads one to conclude that in terms of electronic structure, XPS can easily distinguish U from UO_2, from UF_4 and from UO_3. Unfortunately, the same CANNOT be said for the 5d XAS: the four spectra are difficult to distinguish. The problem with the XAs will be revisited below, after a brief further foray into Photoelectron Spectroscopy.

An internal report:
Electron Spectroscopy of the Oxidation and Aging of U and Pu

Ultraviolet Photoelectron Spectroscopy (UPS) of α-Pu and δ-Pu

    As seen in Figure 2, XPS of the 4f core levels can easily distinguish α-Pu and δ-Pu. So, it is not surprising that Photoelectron Spectroscopy of the Valence Bands can do the same, in terms of the electronic structure of Pu.
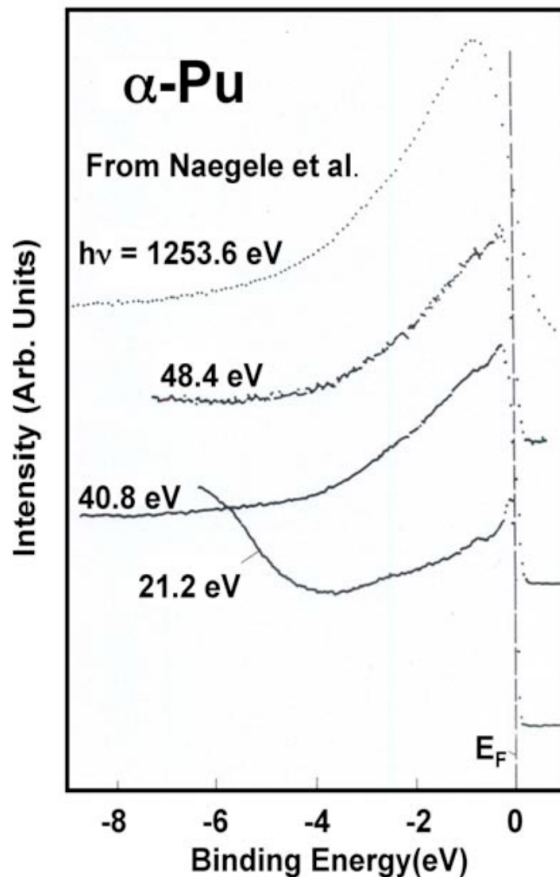

Figure 6a
Valence Band photoelectron spectra of alpha Pu, using He lamp excitation at 21.2 eV, 40.8 eV, and 48.4 eV and Mg Kα excitation (1253.6 eV). [5] E_F is the Fermi Energy at a binding energy of 0 eV. Note the strong similarity of the spectra at low energies.
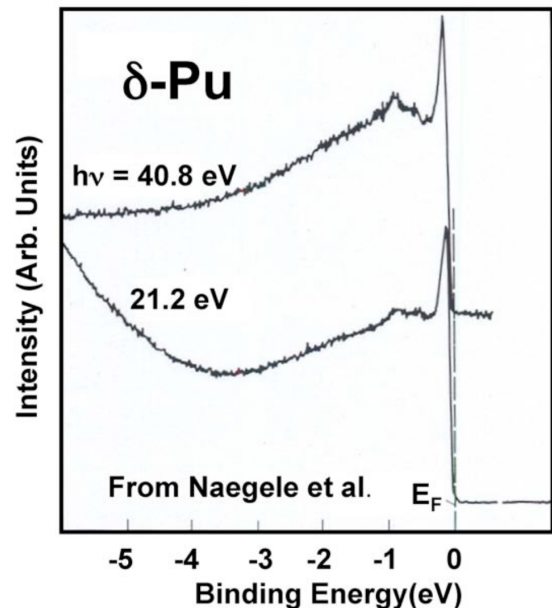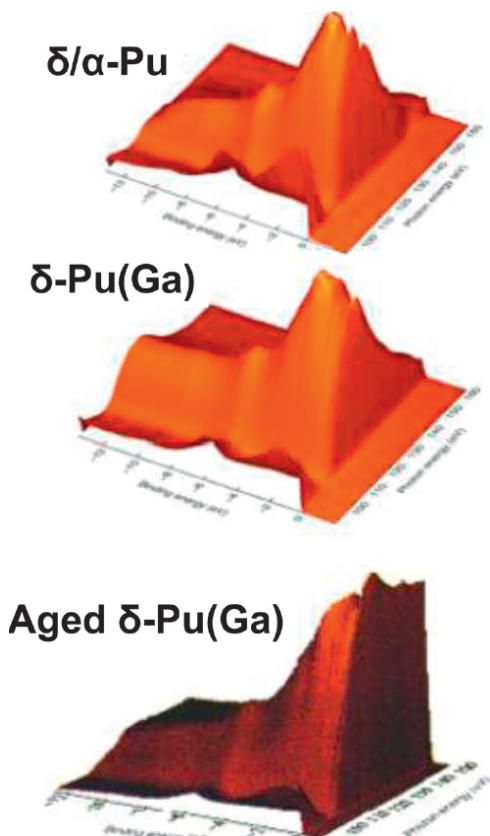

Figure 6b
Valence band photoelectron spectra of delta Pu, using He I (21.2 eV) and HeII (40.8 eV). Again, note the strong similarity of the spectra. [5]

    The topmost spectrum in Figure 6a illustrates a key point: whether using Al Kα (1487 eV) or MgKα (1254 eV) and alpha or delta Pu, the valence band fine structure is lost in the broadening of the Fermi edge and main features near the Fermi Energy. Nevertheless, with UPS the alpha-Pu can be easily distinguished from delta Pu.

An internal report:
Electron Spectroscopy of the Oxidation and Aging of U and Pu

RESPES of Pu

**Resonant Photoelectron
Spectroscopy of Pu**

*Figure 7
Resonant Photoelectron Spectroscopy
(RESPES) data sets are shown here, for a
polycrystalline alpha with a delta-like
surface reconstruction (top), single
crystallite delta (middle), and aged
polycrystalline delta (bottom). [4,27] The
plots show the intensity variations (z axis)
vs. the binding energy of the states (the
negative numbers in eV; zero is the Fermi
energy) and photon energy (between 90
and 160 eV). The bandpass was 100 meV
or less throughout. hv was over the range
of about 90 -160 eV. The binding energy of
the Pu 5d is about 102 eV. The second,
indirect channel for the resonance goes
through the Pu 5d core level. This artwork
is from the cover of Ref. 28.*

In terms of valence electronic structure, RESPES can easily distinguish the new and aged samples of Pu. [4,27,28] It appears that the increase in the resonant behavior is driven by a type of localization associated with aging. In general, more localized systems tend to have stronger resonances. Apparently, radiological aging disrupts the long range order and causes an effective increase in localization. More detail can be found in Ref. 27.

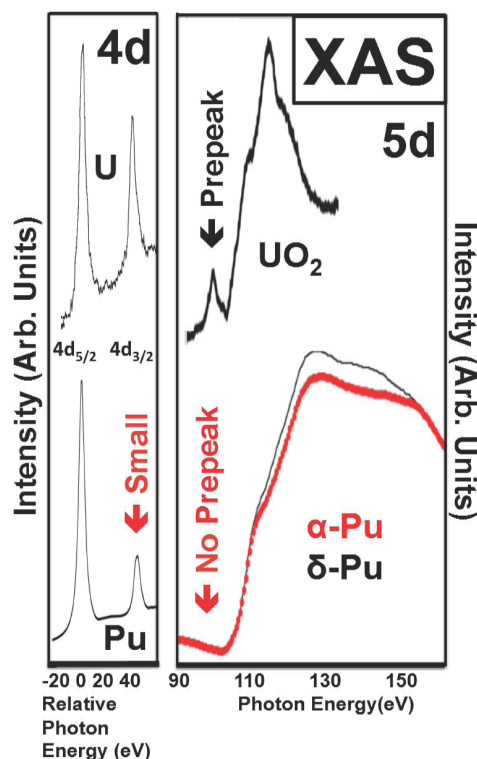**O$_{4,5}$(5d) & N$_{4,5}$(4d) XAS/EELS of U & Pu**

*Figure 8
XAS of the 4d and 5d levels of Pu
and U. See text for details. [29]*

An internal report:
Electron Spectroscopy of the Oxidation and Aging of U and Pu

Now, the XAS spectra of Pu and U will be discussed in detail. [29-31] As demonstrated in Figure 4, the $O_{4,5}$ spectra of U apparently are the same for a wide variety of U materials. In Figure 4, a recent spectrum from UO_2 [30] is shown for comparison. The key point here is that one can easily distinguish the changes in electronic structure between Pu and U, using either the $O_{4,5}$(5d) and $N_{4,5}$(4d) XAS. In the $O_{4,5}$(5d), the U spectra have a pre-peak, while the Pu does not. In the $N_{4,5}$(4d), there is a significant change in relative magnitude of the $4d_{3/2}$ peak that can be used for differentiation. An extended version of this discussion can be found in Ref. 31. The capability to differentiate the elements extends across the lower part of the actinide series, as shown with EELS. [32,33]

Consider again the x-ray absorption spectra of U and Pu shown in Figure 8. [4,7,8,29,31,34,35] The 4d spectrum is from an alpha Pu sample: note the significant change in branching ratio [$B = I_{5/2}/(I_{5/2} + I_{3/2})$], relative to the result for U. While this ratio varies significantly between actinide elements, for Pu the result is fairly independent of chemical or physical state, shown in Figures 9 and 10.

[22,31,36] Within reasonable error analysis, alpha and delta, young and old, all have essentially identical XAS/EELS spectra. It is even questionable whether this measurement can distinguish between metallic and oxidized Pu. Another example of this constancy can be seen in the right panel of Figure 8, where there is a strong similarity between the 5d XAS of alpha and delta Pu. A limitation of the Pu XAS/EELS measurements is the lifetime broadening. The width of the features in the spectra in 8 is intrinsic and cannot be removed, being driven by lifetime broadening. The instrumental contribution in the Pu XAS measurements was 0.1 eV, which is insignificant when compared to the observed line-widths.
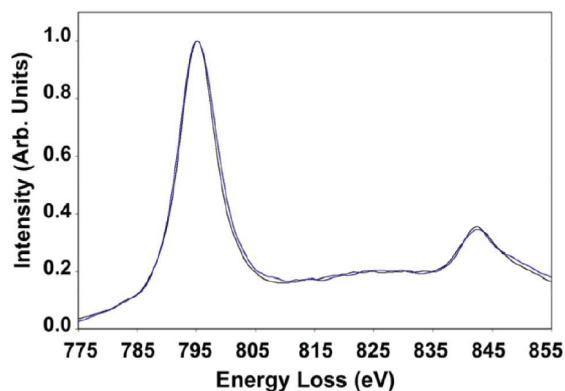

Figure 9
The EELS data for the 4d to 5f transition in α'-Pu and δ-Pu are shown here. α'-Pu is shown in black (dark line) and δ-Pu is shown in blue (light line). Taken from Ref. 31. The two spectra are essentially indistinguishable.
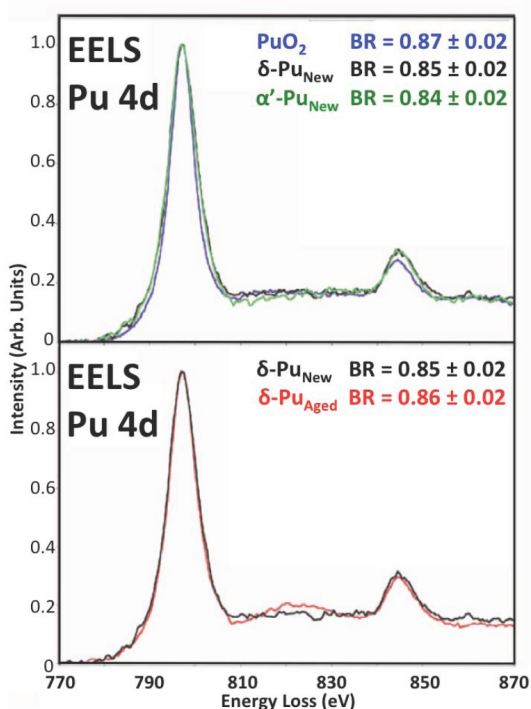
Figure 10 (above)
4d EELS spectra for Pu materials, from Ref. 36. With reasonable error bars, i.e. +/- 0.02, all of these values are essentially the same. [20,22]
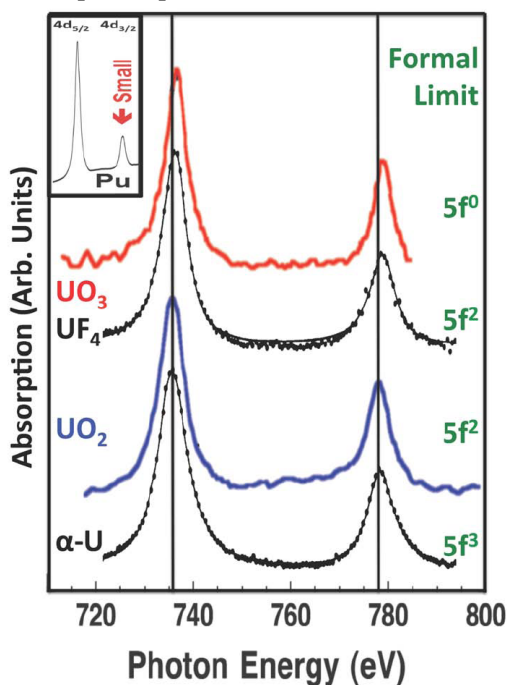
Figure 11(lower left)
X-ray Absorption Spectroscopy data of the $4d_{5/2}$ (near 736 eV) and $4d_{3/2}$ (near 778 eV) peaks of U, UO2, UF4 and UO3 are shown here. [20]

Considering the high degree of localization in Pu, perhaps it is not surprising that the 4d Branching Ratios are invariant. However, even in the far more delocalized U systems, this invariance persists, as shown in Figure 11. The U and UF4 spectra are from Kalkowski et al.[23] The UO2 and UO3 data are from microscopic samples used at the Advanced Light Source. [20] While UO2 and UF4 have the same formal charge limit, it is expected that their oxidation states/ionizations are different, with UF4 being more ionic and less covalent in nature. The inset shows the corresponding peaks for Pu. Thus it appears that while the 4d and 5d XAS measurements are powerful probes of the elemental electronic structure as a function of Z, the nuclear charge, they are insensitive in terms of oxidation and radiological aging.

Figure 11 (above)

An internal report:
Electron Spectroscopy of the Oxidation and Aging of U and Pu

L₃(2p₃/₂) XANES of U and Pu

Now, the case of the $L_3(2p_{3/2})$ X-ray absorption near edge structure of U and Pu will be considered.

Figure 13
Shown here are the Partial Fluorescence Yield (PFY) results for the L₃ X-ray Absorption Near Edge Structure (XANES) measurements. UO₂ and UF₄ are easily distinguishable.

The improvement from the PFY detection carries over to the Pu measurements as well, as can be seen in Figure 14. Note that α-Pu and δ-Pu are easily distinguishable from each other and from the U in Figure 12. Because O and Sb are both chalcogens, the differentiation of Pu and PuSb₂ suggests strongly that PuO₂ and Pu should be distinguishable.
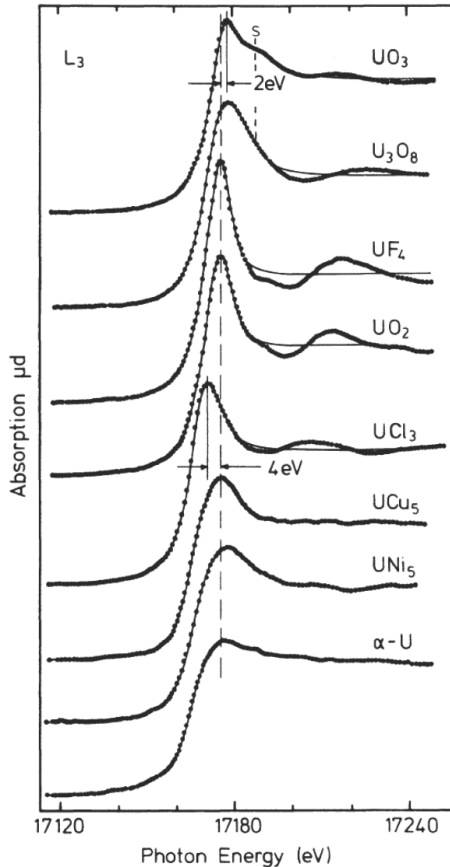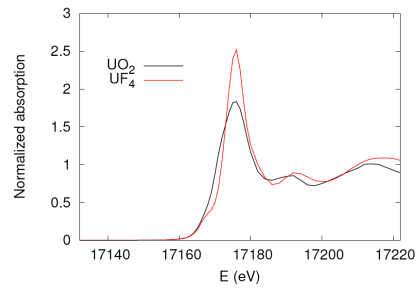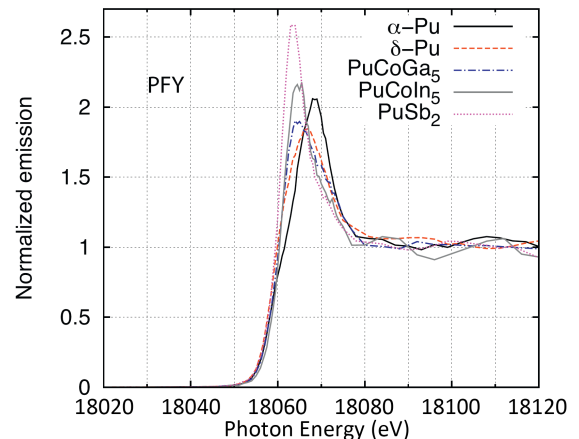

Figure 12
Here is a series of L₃ spectra from U materials, taken from Kalkowski et al. [23] These spectra were collected with conventional detection, with a resolution on the scale of 10 eV. Another good example of this type of data is in Ref. 37.

One can easily distinguish U, UO₂ and UO₃, [23,37] although the better resolution of PFY XANES is required to distinguish UF₄ and UO₂, as shown in Figure 13. [20]

Figure 14
These are L₃ edges of a series of Pu materials collected using the improved (PFY) resolution. Taken from Ref. 12. Also see Ref 11.

Based upon LLNL-JRNL-644374, LLNL-JRNL-636485, LLNL-Conf-475232, LLNL-TR-663216

An internal report:
Electron Spectroscopy of the Oxidation and Aging of U and Pu

BIS, IPES and RIPES of U

Next, the spectra from Bremsstrahlung Isochromat Spectroscopy, Inverse Photoelectron Spectroscopy and Resonant Inverse Photoelectron Spectroscopy will be discussed. Because of the much lower counting rates in Inverse Photoemission relative to Photoemission, a factor of 10,000, the development of the BIS/IPES/RIPES has always lagged behind that of XPS/PES.RESPES. [6] Moreover, because there is no data for Pu systems, the review will be limited to U based materials.

The earliest work, in BIS/IPES on actinide materials, was carried out principally by two groups. The BIS work at hv = 1487 eV was performed by Baer and coworkers, [38,39] while the lower energy IPES (hv near 20 eV) was carried out by Chauvet and Baptist. [40] In Figure 15, the BIS of U from Ref. 38 is compared to a calculation performed by A. Kutepov. [41] The two peak structure in the U UDOS is associated with the spin-orbit split doublet, $U5f_{5/2}$ and $U5f_{7/2}$. Note the strong level of agreement between the experiment and theory. In Figure 16, the BIS collected at hv near 900 eV is shown for UO_2. The data collected with an excitation beam Kinetic Energy (KE) of 915 eV is

essentially the same as that collected at hv = 1487 eV by Baer and Schoenes in 1980. [39] Interestingly, the lower energy IPES data of Chauvet and Baptist shows both a strong peak near the threshold, associated with the U 5f states, and a weaker feature at about 5 to 6 eV above the U5f peak, which has been assigned to the U6d UDOS. [30]
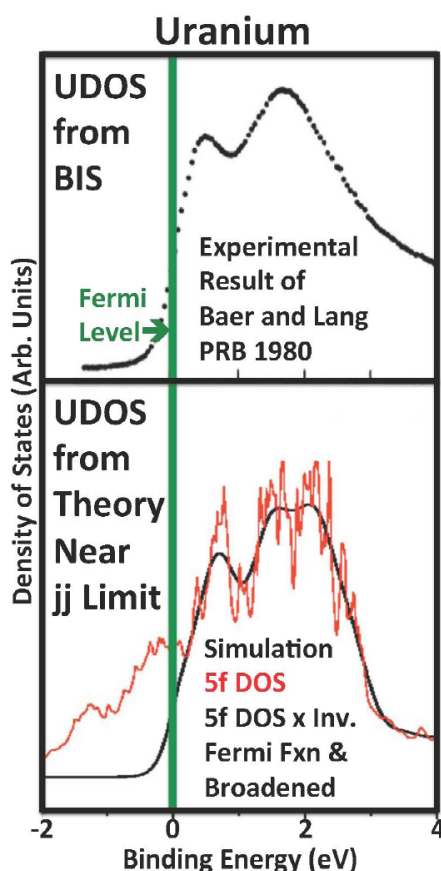

Figure 15
Unoccupied Density of States of U. Top panel: Experimental result is from Bremstrahlung Isochromat Spectroscopy (BIS) by Baer and Lang.[38] Bottom panel: Theory with occupied (neg energies) and unoccupied (pos energies) 5f Density of States U calculated by A.L. Kutepov. [34,41] Taken from Ref. 29.
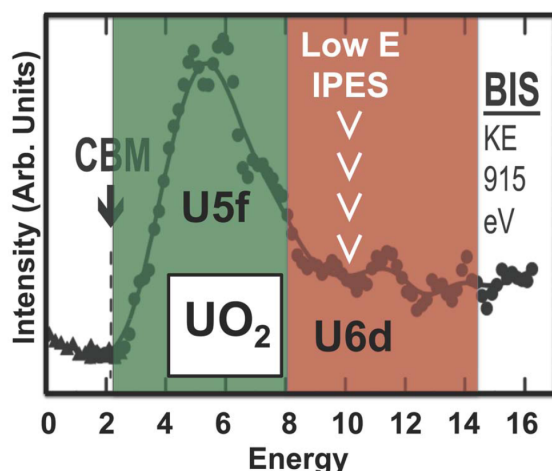
Figure 16
BIS of Uranium Dioxide. A band gap of 2.1 eV is assumed. CBM is conduction band minimum. Neither the spectrum from Baer/Schoenes nor Chauvet/Baptist is shown. From Ref. 29.

Figure 17
RIPES spectra of metallic uranium, showing only a modest increase of intensity at the U N (4d) edge. From Ref. 42.

For the purposes of this paper, it is clear that the BIS of UO_2 is significantly different than that of the BIS of U metal. This demonstration of the distinguishability of U and UO_2 can be further confirmed with a consideration of the RIPES of each, as shown in Figures 17 and 18. Note that the satellite structure in the RIPES of UO_2 is also present in the XES signal as well. [35,42,43]

It has been shown [35,43], that the two peak structure in the RIPES and XES, the main $4d_{5/2}$ peak and the satellite, correspond to the two separate sub-bands in the UDOS shown in Figure 16, that is, the 5f UDOS and the 6d UDOS.
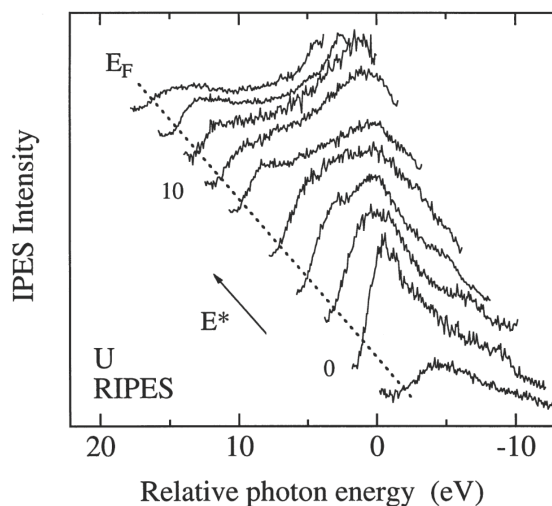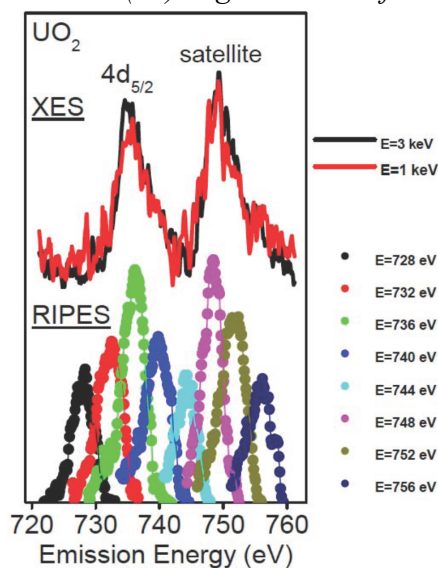

Figure 18
The RIPES and XES of UO_2 is presented here. The XES is shown in the upper part of the figure and the RIPES in the lower part of the figure. Backgrounds have been subtracted. The legend denotes the energy of the excitation, i.e. the incoming electrons. The horizontal scale on the bottom is the energy of the outgoing photons. The resolution bandpass was 2 eV. Note that the satellite is as large as the main peak. [35,43]

An internal report:
Electron Spectroscopy of the Oxidation and Aging of U and Pu

At this point, it is useful to summarize the results so far in a tabular format. This is shown in Table 1 below. The positive answers to the questions are in green, the negative in red. While the Photoelectron Spectroscopy, Inverse Photoelectron Spectroscopy and L_3 XANES provide sensitivity to electronic structural changes with oxidation and radiological aging, the $O_{4,5}(5d)$ and $N_{4,5}(4d)$ XAS & EELS do not. The corresponding figures are also listed.

Table 1

Can the electronic structures of these two materials
be distinguished this technique?

	VB ODOS from XPS, UPS, RESPES	CB 5fUDOS from $O_{4,5}(5d)$ XAS & EELS	CB 5fUDOS from $N_{4,5}(4d)$ XAS & EELS	CB 6dUDOS from $L_3(2p)$ XAS, PFY XANES	CB UDOS from BIS, IPES& RIPES, XES
U vs Pu	Yes Fig.4	Yes Fig. 5,8	Yes Fig. 8	Yes Fig 12,14	
U vs UO_2	Yes Fig.4	Dubious Fig. 5	No Fig.11	Yes Fig. 12	Yes Fig. 15-18
Pu vs PuO_2	Yes Fig. 4		Dubious Fig. 10	Likely Fig. 14	
UO_2 vs UO_3	Yes Fig. 5	Dubious Fig. 5	No Fig. 11	Yes Fig.12	
UO_2 vs UF_4	Yes Fig. 5	Dubious Fig. 5	No Fig.11	Yes Fig. 13	
αPu vs δPu	Yes Fig. 6	Dubious Fig. 8	No Fig. 9,10	Yes Fig. 14	
Rad Damage	Yes Fig. 7		Dubious Fig. 10		

The question then becomes, what steps can be taken to mitigate this problem? Two such approaches will be discussed next.

An internal report:
Electron Spectroscopy of the Oxidation and Aging of U and Pu

Getting past the problems with 5d/4d XAS/EELS: Combining Carefully Calibrated Measurements
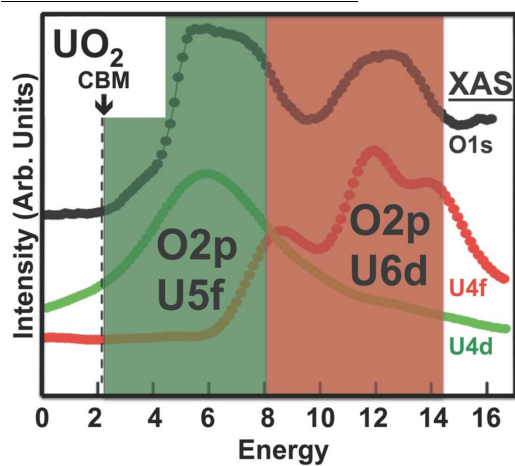

Figure 19
Here is an overlay of XAS spectra, that permits the separation of the UO_2 UDOS into separate U5f-O2p and U6d-O2p sub-bands. [30] A very careful energy calibration is necessary for such overlays. [44] From Ref. 29.

Two alternative approaches to get past the limitations of the 4d/5d XAS/EELS measurements are shown in Figures 19 and 20. In Figure 20a, it is clear that the 3d XAS measurements have the same problems with the 4d/5d. In Figure 20b, Kvashnina and coworkers use a Resonant X-ray Inelastic Scattering (RXIS) experiment to circumvent the lifetime broadening and improve immensely the spectral resolution. See Ref. 45 for further discussion, as well as Ref. 46 for a similar experiment.
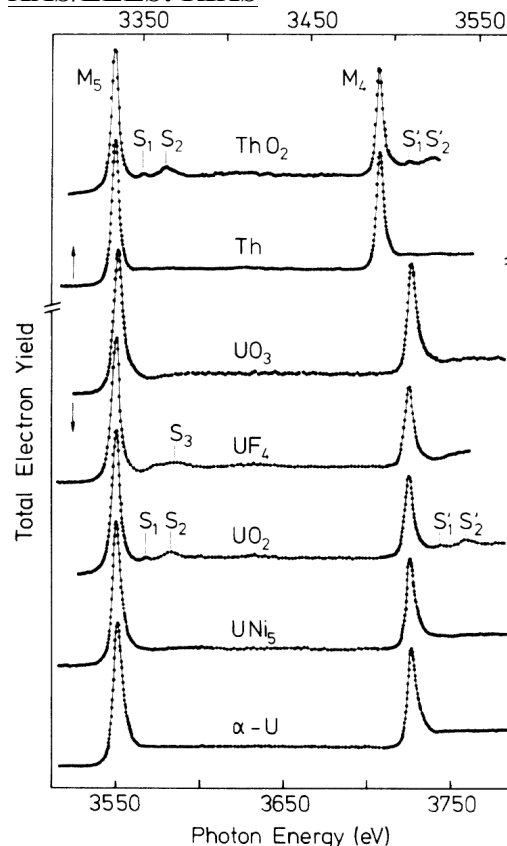
Getting past the problems with 5d/4d XAS/EELS: RIXS

Figure 20a
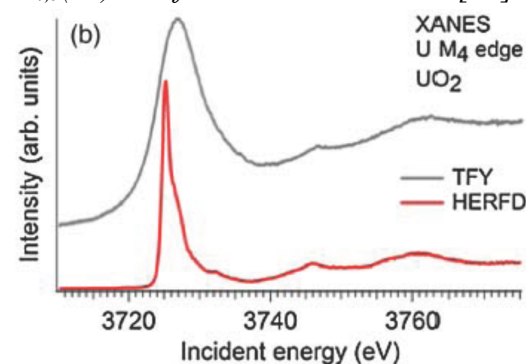*$M_{4,5}(3d)$XAS from Kalkowski et al. [23]*

Figure 20b
Here is a comparison for UO_2 of the conventional M_4 XANES with the results of the high resolution Resonant Inelastic X-ray Scattering experiment. [45] HERFD is high-energy resolution fluorescence detection.

An internal report:
Electron Spectroscopy of the Oxidation and Aging of U and Pu

An internal report:
Electron Spectroscopy of the Oxidation and Aging of U and Pu

References

1. S. D. Drell, Physics Today **53**, 25 (2000).

2. R. Jeanloz, Physics Today **53**, 44 (2000).

3. J.C. Martz and A.J. Schwartz, JOM September 2003, page 19.

4. J.G. Tobin, B.W. Chung, R. K. Schulze, J. Terry, J. D. Farr, D. K. Shuh, K. Heinzelman, E. Rotenberg, G.D. Waddill, and G. Van der Laan, Phys. Rev. B **68**, 155109 (2003).

5. J. R. Naegele, Actinides and some of their alloys and compounds, Electronic Structure of Solids: Photoemission Spectra and Related Data, Landolt-Bornstein Numerical Data and Functional Relationships in Science and Technology, ed. A Goldmann, Group III, Volume 23b, Pages 183 - 327 (1994).

6. J.G. Tobin, "Photoemission and Inverse Photoemission," in "Determination of Optical Properties," Vol. VIII in Physical Methods of Chemistry, 2nd edition, Ed. B.W. Rossiter and R.C. Bretzold, John Wiley and Sons, New York, 1993.

7. K.T. Moore, M.A. Wall, A.J. Schwartz, B.W. Chung, D.K. Shuh, R.K. Schulze, and J.G. Tobin, Phys. Rev. Lett. **90**, 196404 (May 2003).

8. G. van der Laan, K.T. Moore, J.G. Tobin, B.W. Chung, M.A. Wall, and A.J. Schwartz, Phys. Rev. Lett. **93**, 097401 (Aug 2004).

9. K.T. Moore, B.W. Chung, S.A. Morton, S. Lazar, F.D. Tichelaar, H.W. Zandbergen, P. Söderlind, G. van der Laan, A.J. Schwartz, and J.G. Tobin, Phys. Rev. B **69**, 193104 (2004).

10. B.W. Veal, D.J. Lam, H. Diamond and H.R. Hoekstra, Phys. Rev. B **15**, 2929 (1977); B.W. Veal, D. J. Lam, W.T. Carnall and H.R. Hoekstra, Phys. Rev. B **12**, 5651 (1974); B. W. Veal and D. J. Lam, Phys. Rev. B **10**, 4902 (1974); B. W. Veal and D. J. Lam, Phys. Lett. **49A**, 466 (1974).

11. C.H. Booth, Yu Jiang, D.L. Wang, J.N. Mitchell, P.H. Tobash, E.D. Bauer, M.A. Wall, P.G. Allen, D. Sokaras, D. Nordlund, T.-C. Weng, M.A. Torrez, and J.L. Sarrao, Proc. Natl. Acad. Sci. **109**, 10205 (2012).

12. C.H. Booth, S.A. Medling, Y. Jiang, E.D. Bauer, P.H. Tobash, J.N. Mitchell, D.K. Veirs, M.A. Wall, P.G. Allen, J.J. Kas, D. Sokaras, D. Nordlund, T.-C. Weng, J. Electron Spectroscopy and Rel. Phen. **194** 57 (2014).

13. These measurements were made on Beamline 6-2 at SSRL; in collaboration with C.H. Booth, D. Sokaras, T.-C. Weng and D. Nordlund; and using a sample from LANL, provided by E. Bauer.

14. D. Sokaras, T.-C. Weng, D. Nordlund, R. Alonso-Mori, P. Velikov, D. Wenger, A. Garachtchenko, M. George, V. Borzenets, B. Johnson, T. Rabedeau and U. Bergmann, Rev. Sci. Instrum. **84**, 053102 (2013).

15. J. J. Bucher, P. G. Allen, N. M. Edelstein, D. K. Shuh, N. W. Madden, C. Cork, P. Luke, D. Pehl, and D. Malone, Review of Scientific Instruments **67**, 3361 (1996).

16. S. D. Conradson, K. D. Abney, B. D. Begg, E. D. Brady,| D. L. Clark,C. den Auwer, M. Ding,| P. K. Dorhout, F. J. Espinosa-Faller, P. L. Gordon,| R. G. Haire, Nancy J. Hess, R. F. Hess, D. W. Keogh, G. H. Lander, A J. Lupinetti, L. A.

Morales, M. P. Neu, P. D. Palmer, P. Paviet-Hartmann, S. D. Reilly, W. H. Runde, C. D. Tait, D. K. Veirs and F. Wastin, Inorg. Chem. **43**, 116 (2004).

17. S. D. Conradson, B. D. Begg, D. L. Clark, C. Den Auwer, F. J. Espinosa-Faller, P. L. Gordon, N. J. Hess,| R. Hess, D. W. Keogh, L. A. Morales, M. P. Neu, W. Runde, C. D. Tait, D. K. Veirs and P. M. Villella, Inorg. Chem. **42**, 3715 (2003).

18. J. L. Sarrao, L. A. Morales, J. D. Thompson, B. L. Scott, G. R. Stewart, F. Wastin, J. Rebizant, P. Boulet, E. Colineau, and G. H. Lander, Nature **420**, 297 (2002).

19. J. J. Joyce,* J.M.Wills, T. Durakiewicz, M.T. Butterfield, E. Guziewicz, J. L. Sarrao, L. A. Morales, and A. J. Arko, Phys. Rev. Lett. **91**, 176401 (2003).

20. J.G. Tobin, S.-W. Yu, C.H. Booth, T. Tyliszczak, D.K. Shuh, G. van der Laan, D. Sokaras, D. Nordlund, T.-C. Weng, and P.S. Bagus, "Oxidation and Crystal Field Effects in Uranium," submitted to PRB, March 2015.

21. M.T. Butterfield, T. Durakiewicz, E. Guziewicz, J.J. Joyce, A.J. Arko, K.S. Graham, D.P. Moore and L.A. Morales, Surface Science **571**, 74 (2004).

22. J.G. Tobin, J. Electron Spectroscopy and Rel. Phen., **194**, 14 (2014).

23. G. Kalkowski, G. K. Kaindl, W. D. Brewer, and W. Krone, Phys. Rev. B **35**, 2667 (1987).

24. E. Thibaut, J.-P. Boutique, J. J. Verbist, J.-C. Levet and H. Noel, J. Am. Chem. Soc. **104**, 5266-5273 (1982).

25. Yu.A. Teterin, V.A. Terehov, M.V. Ryzhkov, I.O. Utkin, K.E. Ivanov, A.Yu. Teterin A.S. Nikitin, Journal of Electron Spectroscopy and Related Phenomena

114–116, 915–923 (2001).

26. A. Yu. Teterin, Yu. A. Teterin, K. I. Maslakov, A. D. Panov, M. V. Ryzhkov,L. Vukcevic, Phys. Rev. **74**, 045101 (2006).

27. B.W. Chung, A.J. Schwartz, B.B. Ebbinghaus, M.J. Fluss, J.J. Haslam, K.J.M. Blobaum, and J.G. Tobin, J. Phys. Soc. Japan **75**, No. 5, 054710 (May 2005).

28. P. Bagus, R.L. Martin, and J.G. Tobin, ed., Actinide Core Level Spectroscopy and Electronic Structure," J. Electron Spectroscopy and Rel. Phen., Volume 194, (2014).

29. J. G. Tobin, S.-W. Yu, and B.W. Chung, Top.Catal. **56**, 1104(2013).

30. S.-W. Yu, J. C. Crowhurst, J. G. Tobin, S. Sharma, J. K. Dewhurst, P. Olalde-Velasco, W. L. Yang, and W. J. Siekhaus, Phys. Rev. B **83**, 165102 (2011).

31. J.G. Tobin, P. Söderlind, A. Landa, K.T. Moore, A.J. Schwartz, B.W. Chung, M.A. Wall, J.M. Wills, R.G. Haire, and A.L. Kutepov, J. Phys. Cond. Matter **20**, 125204 (2008).

32. M. T. Butterfield, K. T. Moore, G. van der Laan, M. A. Wall, and R. G. Haire, Phys. Rev. B **77**, 113109 (2008).

33. K. T. Moore, G. van der Laan, M. A. Wall, A. J. Schwartz, and R. G. Haire, Phys. Rev. B **76**, 073105 (2007).

34. J.G. Tobin, K.T. Moore, B.W. Chung, M.A. Wall, A.J. Schwartz,   G. van der Laan, and A.L. Kutepov, Phys. Rev. B **72**, 085109 (2005).

35. J.G. Tobin and S.-W. Yu, Phys. Rev. Lett, **107,** 167406 (2011).

36. K. T. Moore, G. van der Laan, R. G. Haire, M. A. Wall, and A. J. Schwartz, Phys.

Rev. B **73**, 033109 (2006).

37. S. Van den Berghe, M. Verwerft, J.-P. Laval, B. Gaudreau, P. G. Allen, A. Van Wyngarden, J. Solid State Chem. **166**, 320 (2002).

38. Y. Baer and J.K. Lang, Phys. Rev. B **21**, 2060 (1980).

39. Y. Baer and J. Schoenes, Solid State Commun. **33**, 885 (1980).

40. G. Chauvet and R. Baptist, Solid State Commun. 43, 793 (1982).

41. M.T. Butterfield, J.G. Tobin, N.E. Teslich Jr, R.A. Bliss, M.A. Wall, A.K. McMahan, B.W. Chung, A.J. Schwartz, and A.L. Kutepov, Matl. Res. Soc. Symp. Proc. **893**, 95 (2006).

42. M. Grioni P. Weibel, M. Hengsberger, Y. Baer, J. Electron Spectrosc. Rel. Phenom. **101–103**, 713 (1999).

43. S.-W. Yu and J.G. Tobin, J. Electron Spectroscopy and Rel. Phen., **187**, 15 (2013).

44. S.-W. Yu, J. G. Tobin, P. Olalde-Velasco, W. L. Yang, and W. J. Siekhaus, J. Vac. Sci. Tech. **A 30**, 011402 (2012).

45. K.O. Kvashnina, S.M. Butorin, P. Martin and P. Glatzel, Phys. Rev. Lett. **111**, 253002 (2013).

46. J. A. Bradley, S. S. Gupta, G. T. Seidler, K. T. Moore, M. W. Haverkort, G. A. Sawatzky, S. D. Conradson, D. L. Clark, S. A. Kozimor, and K. S. Boland, Phys. Rev. B **81**, 193104 (2010).